Veterinary Pathology
2024, Vol. 61(5) 815–828

DOI: 10.1177/03009858241238685
journals.sagepub.com/home/vet


Pathology of "double scale" skin defect in farmed American alligators (*Alligator mississippiensis*) and the possible association with hepatic fibrosis

Ilaria M. Piras[1], Annemarie Bezuidenhout[2], Josué Díaz-Delgado[3,4], Deirdre Slawski[2], and Pamela A. Kelly[1]

Abstract

"Double scale" is a poorly characterized skin defect of crocodilians that drastically reduces the economic value of crocodilian skin. This study investigated the morphology and pathogenesis of double scale in a ranching farm of American alligators (*Alligator mississippiensis*). We compared the histopathology of skin and selected organs (liver, lung, kidney, heart, spleen, intestine, and brain) of alligators with double scale against healthy control animals, together with serum and liver vitamin and mineral levels. Skin affected with double scale had statistically significant hyperkeratosis, epidermal atrophy, and increased basal cell degeneration compared with control alligators ($P < .0001$). Interestingly, all alligators with double scale had varying degrees of hepatic fibrosis. Feed analysis showed that alligators that had double scale and hepatic fibrosis had prolonged dietary exposure to high levels of vitamin A, iron, and copper. Serum analysis indicated that levels of zinc ($p < .0001$), copper ($P < .05$), and vitamin E ($P < .002$) were significantly lower in alligators with hepatic fibrosis and double scale compared with controls. Finally, immunohistochemical analysis of skin with double scale showed a marked reduction in immunolabeling with the zinc-binding protein metallothionein. These results suggest that zinc deficiency, in combination with other micronutrient anomalies, may play a role in the pathogenesis of double scale in alligators with liver fibrosis.

Keywords

American alligator, *Alligator mississippiensis*, double scale, hepatic fibrosis, vitamin A, zinc deficiency

After decades of unregulated and intensive hunting for skin exploitation, most crocodilian species became endangered, and some were almost extirpated by the beginning of the 1970s.[39] This dramatic decline of wild crocodilian populations induced several countries to protect crocodilians through legislation. In addition, the worldwide trade of wild species and their products became regulated by the Convention on International Trade in Endangered Species (CITES) from 1975. Crocodile farming gained momentum in this historical context as a valuable opportunity to provide skins for an ever-growing leather market and, at the same time, incentivize the conservation of crocodilians.[22,23]

Ranching is the most common way of farming American alligators (*Alligator mississippiensis*) in the United States. Ranching farms are intimately connected to the natural alligator habitat and have a significant impact in wildlife conservation. This method of production is based on the collection of wild eggs, followed by regular reintroduction of juveniles and hatchlings born on farms, to maintain the wild crocodilian population.[27] This practice incentivizes the preservation of the wet land habitats, saves eggs that are often subject to predation or destruction in wild conditions,[37] and boosts hatchlings survival until adulthood.[5,6,25,37]

The main focus of crocodile farming is to produce high quality skins to supply the expanding demand for premium hides for the luxury leather market.[6] For this reason, care is taken during rearing to minimize damage to the belly skin, which is the most valuable part of the hide, from abrasive surfaces, interactions with other crocodiles, and from any dermatologic conditions that can produce a defect.[6,14,28]

This study is a clinical and pathological investigation conducted on a ranching farm of American alligators following a year of poor skin gradings due to high incidence of "double scale" (DS) defects in the population. This skin condition reduces leather quality and has an important impact on the financial sustainability of the industry. The histopathology of

[1]University College Dublin, Dublin, Ireland
[2]Padenga Holdings Ltd, Harare, Zimbabwe
[3]Texas A&M Veterinary Medical Diagnostic Laboratory, College Station, TX
[4]University of Surrey, Guildford, UK

Supplemental Material for this article is available online.

Corresponding Author:
Pamela A. Kelly, School of Veterinary Medicine, University College Dublin, Belfield, Dublin 4, D04 V1W8, Ireland.
Email: Pamela.Kelly@ucd.ie

Figure 1. Crust tan leather with double scale defect, American alligator. The anatomic area depicted is the transition between the belly (on the left) and the flank skin (on the right). Most scales have a central circular indentation (arrowheads) that confers a doubled appearance to the appendages.

this condition remains uncharacterized, and the etiology is unclear. The condition received its name from the duplicated appearance of scales following chemical and physical removal of all skin tissue components except collagen (crust tan hide) and also in tanned hides (Fig. 1). Multifactorial causes involving potential nutritional, metabolic, and genetic factors have been considered anecdotally, but none have been explored in the scientific literature so far.

The aims of this study were to characterize the gross and histopathologic features of DS skin lesions and to investigate the possible causes of the disorder. To achieve this, 2 cohorts of alligators were assessed. The first cohort ("DS 2018 cohort"), hatched in 2017 and 2018, had a high incidence of DS, while the second ("Control 2019 cohort"), hatched in 2019, was free of DS and acted as the control group. Both cohorts were hatched and raised in the same facility under similar farming conditions, with the exception of being fed different commercially available formulated diets.

Materials and Methods

Animals

This study was reviewed by the Animals in Research Ethics Committee in University College Dublin and was deemed full ethics review exempt (AREC-E-22-20-KELLY) as it involves samples collected exclusively during normal husbandry or veterinary clinical procedures. No procedures were carried out on live animals and no animal was euthanized for the sole purpose of this study.

All alligators included in this study were reared on the same farm in Texas. At the time of investigation, the farm produced over 12,000 animals per annum on a single site from wild caught eggs that hatched in captivity. Animals were housed in groups of 20–80 depending on their size. These groups consisted of a mix of both male and female alligators. The houses were insulated and divided into pools and feeding and basking decks. Pool water was kept at a constant temperature range of 29–32°C. Diets consisted of commercially available complete crocodilian pelleted feed purchased from a single manufacturer that was tested routinely in-house for mycotoxins using CHARMS Rosa-M Reader (Lawrence, Massachusetts).[2] In addition, feed samples were regularly submitted to Eurofins Scientific Inc. (Des Moines) for mycotoxin testing (PQA07 Mycotoxins 6 Package: alfatoxin, fumonisin, ocharatoxin, T-2/HT-2 toxin, zearalenone).

Feed Analysis

Two feed stocks were used in this study. One feed stock was used in 2017–2018 (Feed 2018) to feed animals who hatched in 2017 and 2018 (DS 2018 cohort). Under suspicion of a nutritional imbalance and following feed analysis the feed was changed in January 2019. Animals hatched in 2019 (Control 2019 cohort) were fed exclusively with 2019 feed stock (Feed 2019).

A total of 19 samples of dry pelleted feed used in 2017 and 2018 (Feed 2018) were assessed by Eurofins Scientific Inc. (Des Moines), and 21 samples from the feed stock used during 2019 and 2020 (Feed 2019) were analyzed at Midwest Laboratories (Omaha) using high-performance liquid chromatography.

For vitamin A quantification, sample aliquots were saponified with ethanolic potassium hydroxide in the presence of butylated hydroxytoluene. The mixture was extracted with hexane. The combined hexane phases were washed with water and dried over sodium sulfate. The concentration of retinol in the hexane extract was determined using high-performance liquid chromatography with a silica column and fluorescence detector. For quantification of the beta-carotene content, the solvent was exchanged to 25% tert-butyl methyl ether in methanol before injection on a high-performance liquid chromatography equipped with a C30 Carotenoid column and ultraviolet (UV)-visible spectroscopy detector.

For vitamin E, sample aliquots were saponified with ethanolic potassium hydroxide in the presence of ascorbic acid. The mixture extracted with a petroleum ether/ethyl acetate solution. The combined organic phases were washed with water and dried over sodium sulfate. The solvent was exchanged with hexane before using high-performance liquid chromatography with a silica column and fluorescence detector.

Metals were digested using dry ashing. The resultant digest was analyzed by inductively coupled plasma optical emission spectrophotometry against a set of ISO-certified standards. The specific method used for each analyte is listed in Supplemental Table S1.

Sample Collection

Between April 2019 and June 2020, during routine harvest at the abattoir, samples of liver, lung, kidney, heart, spleen, intestine, brain, and free catch blood obtained at bleeding were collected from 85 randomly selected alligators (48 from DS 2018

cohort and 37 from Control 2019 cohort) (Supplemental Table S2). The tissue samples were collected in formalin and 49 fresh samples of liver (27 from DS 2018 cohort and 22 from Control 2019 cohort) were also frozen. Serum was obtained from 42 samples (20 from DS 2018 cohort and 22 from Control 2019 cohort) of the free catch blood and was frozen. From DS 2018 cohort, belly skin sample were collected from all animals presenting with DS defects (18 samples, 38% of alligators) and 9 samples of normal belly skin were sampled from Control 2019 cohort, which were free of DS defects (Supplemental Table S2). All skin samples were formalin-fixed. The age range for selected animals was between 9 and 19 months; sex and farming pen of origin were mixed. The average length and belly width for each age group of alligator at harvest is presented in Supplemental Table S3. As factors, such as skin quality and market demand influence when an alligator is harvested, a direct size comparison between the 2 cohorts was not possible.

Histopathology

Following fixation in 10% neutral-buffered formalin, tissues were processed and embedded in paraffin, sectioned at 4 μm, and stained with hematoxylin and eosin. Histological sections were assessed blind and independently for the presence of histopathological changes by pathologists PAK (ECVP board certified), JDD (ACVP board certified), and IMP (anatomic pathology resident).

Of the 18 belly skin samples from alligators that had gross evidence of DS (DS 2018 cohort), 61 scales were obtained for histological examination. Of the 9 belly skin samples from alligators that showed no evidence of DS (Control 2019 cohort), 32 scales were assessed. Image software ImageJ was used to carry out skin measurements on 36/61 (59%) scales affected with DS (2 scales per DS 2018 cohort alligator) and 18/36 (50%) scales from those with normal scales (2 scales per Control 2019 cohort alligator). For the measurements, microphotographs at 200× magnification with scale set to 15 μm (equivalent to alligator erythrocyte diameter) were used. The corneal layer and the live strata of the epidermis, which includes strata basale and spinosum and the transitional layer, were measured at center of the scale. For each scale, 3 measurements were taken, and the average was used as the final value. Six representative samples of skin, 3 normal and 3 with DS defect were also stained with Gordon and Sweet's reticulin and used for immunohistochemical labeling.

Based on examination of hematoxylin and eosin sections, 3 representative samples of liver from the Control 2019 cohort alligators and 3 samples of liver from DS 2018 cohort alligators were selected for staining with Masson's trichrome, Gordon and Sweet's reticulin, and Perls' Prussian blue stains to highlight collagen, reticular fibers, and iron, respectively. Periodic acid-Schiff reaction was also carried out to highlight carbohydrate content within hepatocytes. The same liver samples were used for immunohistochemical labeling.

The liver changes were measured based on the severity of hepatocyte vacuolation, biliary proliferation, and fibrosis. Briefly, hepatocyte cytoplasmic vacuolation was scored on scale of 0–4 (0 = absent, 1 = hepatocytes have finely vacuolated to wispy eosinophilic cytoplasm with no increase in cell size, 2 = hepatocytes have finely vacuolated (vacuoles larger than score 1) eosinophilic cytoplasm with no increase in cell size, 3 = hepatocytes have prominent clear cytoplasmic vacuoles and a conspicuous increase in cell size, 4 = hepatocytes have prominent large clear cytoplasmic vacuoles with an obvious increase in cell size).[44] Biliary proliferation was scored on a scale of 0–4, counting bile duct profiles per 10 triads (0 = maximum of 14 bile ducts/10 triads; 1 = 15–20 bile ducts/10 triads; 2 = 21–30 bile ducts/10 triads; 3 = 31–50 bile ducts/10 triads; 4 = > 50 bile ducts/10 triads). Severity of fibrosis was scored on a scale of 0–4 based on the percentage of periportal collagen deposition increase relative to normal using 100× magnification (0 = absent, 1 = up to 10%, 2 = up to 20%, 3 = up to 30%, 4 = presence of bridging fibrosis). Histology score for normal liver was considered to be 0 for hepatocyte vacuolation, biliary proliferation, and for fibrosis. The value assigned to each liver was an average of the independent scoring evaluations made by each pathologist.

Immunohistochemistry

For validation of immunohistochemistry assay specificity in American alligator tissues, we designed positive and negative tissue controls for each antibody used.[43] Fibrogenic cells were assessed by immunohistochemistry on 6 liver samples, 3 from the Control 2019 cohort and 3 from the DS 2018 cohort, using a mouse monoclonal antibody to human desmin (1:25, clone D33, M0760; Dako, Denmark A/S) and a mouse monoclonal antibody to the alpha isoform of human smooth muscle actin (α-SMA) (1:100, clone 1A4, n M0851; Dako, Denmark A/S). Alligator skeletal muscle was used as positive control for antidesmin antibody; the tunica muscularis of alligator intestines served as positive control for α-SMA antibody. For both antibodies, one reaction with mouse immunoglobulin G (IgG) antibody serum was included as a negative control. All tissues were fixed in 10% neutral-buffered formalin, processed, and embedded in paraffin. Tissue blocks were then sectioned at 4 μm and sections mounted on charged glass slides. Antigen retrieval for desmin and α-SMA consisted of treatment of the tissue sections with sodium citrate buffer (pH = 6) in a Menarini access retrieval unit under full pressure at 125°C for 1 minute, 40 seconds. Since we lacked frozen samples of skin, the presence of zinc deficiency was assessed targeting metallothionein (MT) with a rabbit polyclonal antimouse MT (1:400, ab192385, Abcam, UK) on 6 samples of alligator skin, 3 with DS defect (DS 2018 cohort), and 3 normal (Control 2018 cohort). Mouse skin was used as positive control for the primary antibody. One reaction with rabbit IgG antibody serum was included as a negative control. Tissue sections were treated with protease for antigen retrieval. The detection method for all antigens in this study was horseradish peroxidase with 3,3′-diaminobenzidine as the chromogen.

Vitamin A, Vitamin E, and Mineral Concentration in Liver and Serum

A total of 49 frozen liver samples, including 27 from DS 2018 cohort and 22 from Control 2019 cohort were assessed for concentrations of copper, iron, zinc, manganese, molybdenum, cobalt, arsenic, cadmium, lead, thallium, selenium, vitamin E, retinol, palmitate, and total vitamin A by inductively coupled plasma mass spectrometry and chromatography at Texas A&M Veterinary Medical Diagnostic Laboratories. The same laboratory determined copper, iron, zinc, manganese, molybdenum, cobalt, arsenic, cadmium, lead, thallium, selenium, and vitamin E concentrations on 42 samples of frozen serum (20 from DS 2018 cohort and 22 from Control 2019 cohort).

Metals and minerals were all assayed on inductively coupled plasma mass spectrometry, each element with its own standard curve of at least 5 points with correlation coefficient greater than 0.995. All samples were diluted using an internal standard solution whose performance was monitored. Elemental concentrations were reported on a dry matter basis. Samples whose mass was measured to the nearest 0.0001 g were dried to constant weight in a convection oven at 95°C and reweighed to determine dry weight fraction. For each animal, a liver aliquot of approximately 0.5 g was digested using 5.00 ml ultrapure nitric acid, 0.25 ml ultrapure hydrochloric acid, and 1 ml 30% hydrogen peroxide. Samples were diluted to 50 ml with tissue diluent containing internal standard and were transferred to the inductively coupled plasma mass spectrometry.

Vitamin A, retinol, palmate, and vitamin E were assayed by chromatography performed on a Waters system using a C18 Cosmosil PBr column (4.6 × 250 mm) and mobile phases acetonitrile and 0.1 % acetic acid in a gradient with UV monitoring at 350 nm for vitamin A. In a darkened room in a biological safety cabinet, an approximately 1 g aliquot of each animal sample (measured to the nearest 0.01 g) was homogenized in de-gassed, deionized water with a final added volume of 5 ml. Beta-hydroxybutyrate in ethanol was added and samples were subjected continuous rotation at approximately 30 rpm for 20 minutes. Each tube then received 2 ml hexane and was recapped and rotated for another 20 minutes. After centrifugation at approximately 2500 rpm to ensure separation of phases, 1 ml of each hexane layer was evaporated to dryness under nitrogen. Resuspension in acetonitrile was followed by filtration at 0.45 μm into chromatography vials.

Statistical Analysis

Vitamins and mineral levels from liver and serum of animals with liver fibrosis (DS 2018 cohort) were compared with the results of control animals (Control 2019 cohort).

Results of feed analysis between Feed 2018 and Feed 2019 were also compared.

GraphPad Prism 9.3.0 (GraphPad Software for macOS, San Diego, California USA, www.graphpad.com) was used for statistical analyses. Normality of distributions was verified by means of Anderson-Darling test. For comparison between 2 groups, Student's *t*-tests or Mann-Whitney tests were performed for parametric and nonparametric analyses, respectively. For comparison between parametric and nonparametric data sets, a Student's *t*-test was performed in case skewedness of nonparametric measures was between 1 and –1. Differences were considered significant for $P < .05$. Pearson's correlation coefficient was computed to assess relationship between hepatic concentrations of iron and vitamin A and the severity of liver pathology, which was measured using the histological scores detailed above.

Results

Gross and Histological Characterization of "Double Scale"

DS presented grossly as a combination of focally extensive pitting and roughening of the cranial and medial edge of the belly scale (18/18, 100%), mostly accompanied by a brown discoloration (Fig. 2a). In the most severe cases, a linear, ring-shaped indentation within the central portion of the scale was also present (7/18, 39%) (Fig. 2a). Histologically, indentation presented as a depression of the epidermis and superficial dermis (Fig. 2b), while the pitting and roughening of the scales consisted of keratin fragmentation (Fig. 2c). Furthermore, there was an increased number of degenerating basal keratinocytes, mean = 3.7 per 10,000 cells, standard deviation (SD) = 9.3, $n = 19$, (Fig. 2d) compared with normal scales (mean = 0.21 per 10,000 cells, SD = 0.39, $n = 9$). Marked orthokeratotic hyperkeratosis affecting the β- and α-keratin layers of the scale characterized all DS samples examined (18/18, 100%) compared with normal scales (Fig. 3). Associated with hyperkeratosis, there was a significant thinning of the live strata of the epidermis, including the basal, supra-basal, and transitional layers (Fig. 3). The β-keratin layer thickness was 94.6 μm on average in normal scales (SD = 11.6, $n = 18$) and 168.5 μm in DS (SD = 35.4, $n = 36$, P value $< .0001$) (Fig. 4a). The α-keratin layer, was an average of 18.8 μm (SD = ±5.3, $n = 18$) in normal scales and an average of 70.5 μm (SD = 21.5, $n = 36$, P value $< .0001$) in DS (Fig. 4b). The live strata of the epidermis was an average of 51 μm thick in normal scales (SD = 11.9, $n = 18$) and an average of 33.1 μm thick in DS (SD = 9.9 μm, $n = 36$, P value $< .0001$) (Fig. 4c). In addition, several DS scales exhibited disarray of collagen fibers (9/19; 47%) and a multifocal increase in the ground substance of the dermis (Fig. 5). Collagen disarray was not detected in any of the scales from controls (Control 2019 cohort).

Histopathological Examination of Visceral Organs

Histopathological examination was carried out on tissues from 85 animals (48 DS 2018 cohort and 37 Control 2019 cohort) including samples of liver, intestine, lung, heart, brain, spleen, and kidney. Thirty-one of the 37 liver samples from the Control 2019 cohort were considered normal (Fig. 6a–c), showing no evidence of fibrosis, bile duct proliferation, or hepatocyte

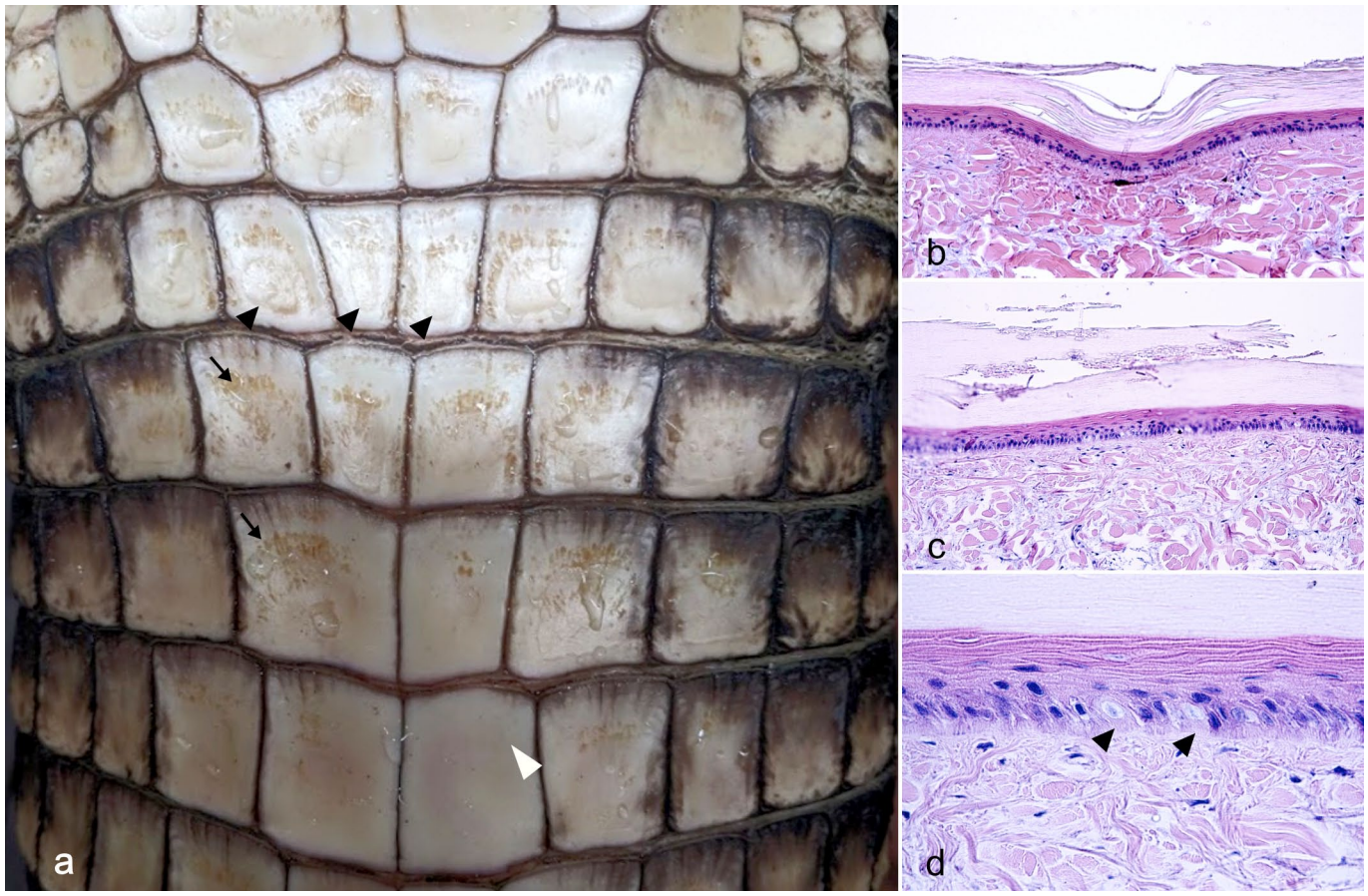

Figure 2. Belly skin with double scale defect, American alligator. (a) Gross appearance of double scale defect characterized by a rough and pitted surface (arrows) often associated with a linear dent (black arrowheads). Note the smooth and even surface of the normal scale (white arrowhead). (b) The dent is histologically characterized by a focal depression of the epidermis and the dermis. Hematoxylin and eosin (HE). (c) The rough surface is characterized histologically by a fragmented corneal layer. HE. (d) Higher magnification of the epidermis shows frequent degeneration of the basal keratinocytes (arrowheads). HE.

vacuolation (score 0) (Fig. 6b, d, and f). While 2 liver samples presented mild hepatocyte vacuolation (score 1) and 4 had mild bile duct proliferation (score 1) (Supplemental Table S2). No significant changes were found in the other organs assessed.

All 48 liver samples from the DS 2018 cohort had pathologic changes (48/48; 100%). The severity of liver disease was quantified using a scoring system based on the presence and extent of liver fibrosis, biliary duct proliferation, and hepatocyte vacuolation. Details of the scoring system are outlined above in Materials and Methods and Supplemental Figure S1. In 33 of 48 (69%) cases, liver disease was characterized by fibrosis of variable severity (scores 1–4) (Fig. 6b and Supplemental Figure S1). Hepatic fibrosis formed largely around periportal tracts and adjacent to the liver capsule. In the most severe cases, fibrosis bridged several portal areas resulting in complete loss of normal lobular architecture and concomitant hepatocellular nodular hyperplasia (regeneration) (Fig. 6b, d). Bile duct proliferation (scores 1–4) (Fig. 6a) and glycogen accumulation (scores 1–4) causing hepatocyte vacuolation and cell swelling, were also evident in all samples (48/48, 100%) (Fig. 6f). There was a subjective increase in the number of periportal melanomacrophage (or pigment) centers compared with samples from the Control 2019 cohort (Fig. 6a, b). All 18 of the animals that had gross and histological evidence of DS also had histological evidence of liver fibrosis, bile duct proliferation, and hepatocyte vacuolation.

Liver and Serum Oligoelements and Vitamin Analysis

Vitamin and mineral levels from the livers and serum of animals with liver fibrosis and normal livers are summarized in Table 1, together with the results of statistical analyses between means (or medians) of the 2 groups. Hepatic levels of known hepatotoxins, such as vitamin A (880.6 μg/g, P value $< .0001$) and iron (734.6 μg/g, P value $< .0001$) were significantly increased in livers with fibrosis compared with controls (vitamin A = 389.8 μg/g; iron = 388.2 μg/g). Copper levels were also increased (57.92 μg/g vs 39.36 μg/g of controls), but the difference between livers with fibrosis and controls was not statistically significant. There was a strong positive correlation between severity of liver disease and levels of hepatic iron (Pearson's $r = .51$, P value $< .0001$) and vitamin A (Pearson's

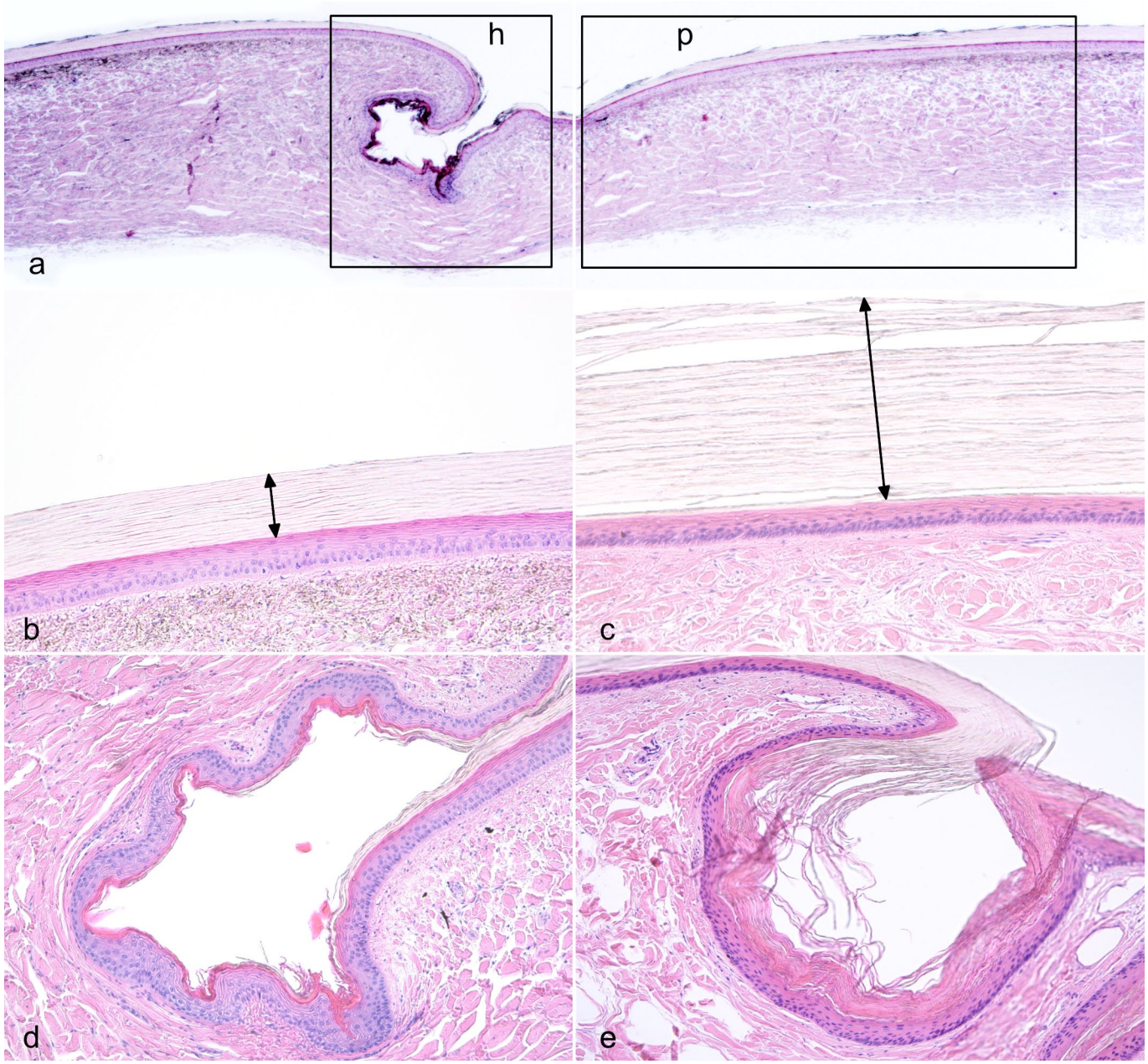

Figure 3. Histologic features of double scale (DS), American alligator, skin. (a). Normal anatomy of alligator scales showing the plate region (p box) constituting most of the scale and the hinge region (h box). The cranial scale is on the left and the caudal scale is on the right. Hematoxylin and eosin (HE). (b) Higher magnification view of the plate region of a normal scale. Note the β-keratin covering the plate of the scale stains negatively (double arrow). HE. (c) The keratin layer of skin affected with DS is markedly thickened at the level of the plate (double arrow) while the live strata of the epidermis is thinner compared with normal scales. HE. (d). Higher magnification view of the hinge region of a normal scale. The α-keratin at the level of the hinge stains pink with eosin. (e) The α-keratin at the level of the hinge is markedly thickened in DS. HE.

$r = .49$, P value $< .0001$) (Supplemental Figures S1f and S1g). Hepatic levels of zinc were also significantly increased while manganese was significantly lower in livers with fibrosis compared with controls. Serum of alligator with liver fibrosis had significantly decreased levels of zinc, copper, and vitamin E, while manganese was significantly higher compared with controls. (Fig. 9).

Feed Analysis

Feed analysis highlighted differences in concentration of total protein, total fat, total fiber, iron, copper, zinc, manganese, calcium, and vitamin A between Feed 2018 and Feed 2019. In detail, the concentration of fiber (1.3%), fat (14.6%), and protein (55 %) in Feed 2019 were significantly increased

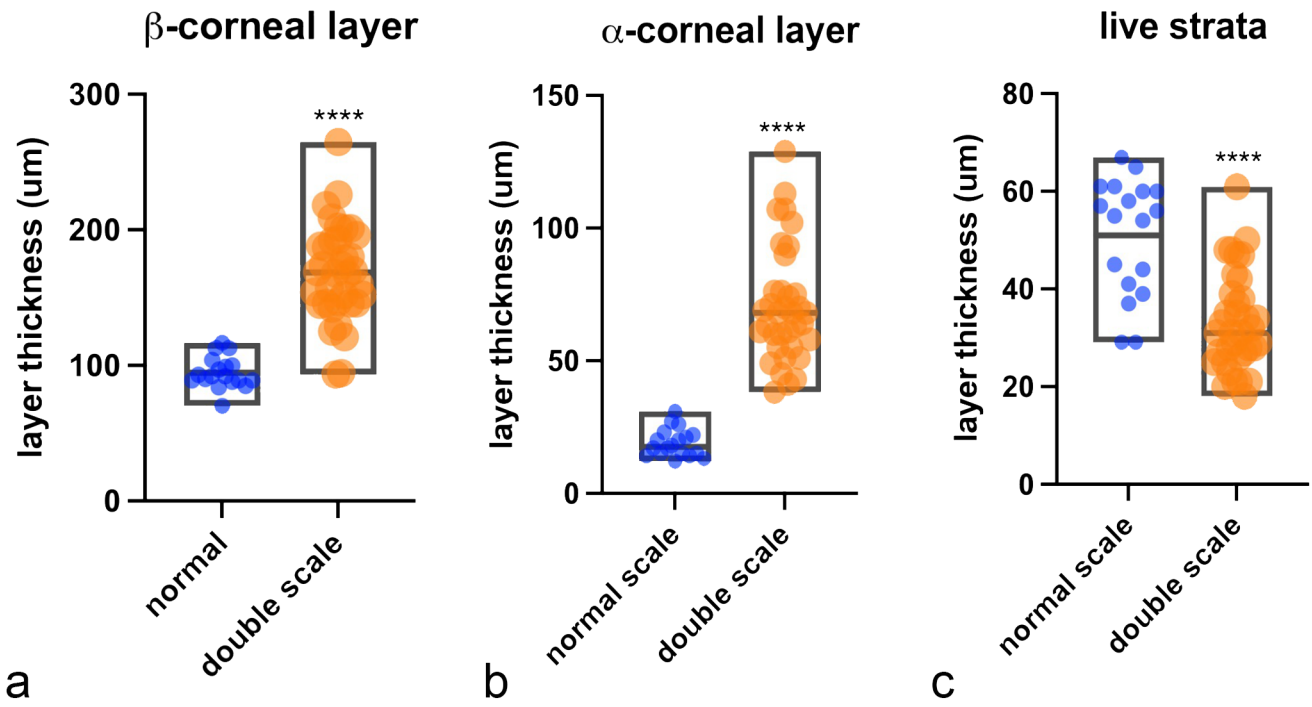

Figure 4. Comparison between epidermal thickness of normal scales and double scales (DS). The box graphs show measurements of (a) β-keratin layer, (b) α-keratin layer, and (c) epidermal live strata of normal (n = 18 measurements) and DS (n = 38 measurements). Central line in the box indicates mean. Difference of means calculated by Student's t-test was significant, P value < .0001 (****).

compared with Feed 2018 (fiber 0.7%, P value < .0021; fat 6.9%, P value < .0001; protein 50%, P value < .0001). While the concentration of vitamin A (1521 IU/100 g), iron (605 ppm), copper (20 ppm), manganese (78 ppm), zinc (236 ppm), and calcium (1.82 %) was significantly decreased (P value < .0001) in Feed 2019 compared with Feed 2018 (vitamin A = 3193 IU/100 g, iron = 1197 ppm, copper = 36 ppm, manganese = 133 ppm, zinc = 373 ppm, calcium = 2.85%). Results of feed composition for each stock feed (Feed 2018 and Feed 2019) and statistical analysis are available in Table 2.

Immunohistochemistry

Alligator rhabdomyocytes and intestinal tunica muscularis smooth muscle cells were labeled by antidesmin and α-SMA antibody, respectively (positive controls) (Supplemental Figures S2a and S2b). Immunolabeling for α-SMA in normal liver samples highlighted the diffuse presence of low numbers of spindle-shaped cells stretching into the perisinusoidal spaces and in the periportal areas (Fig. 7a). Livers with fibrosis exhibited a subjective marked increase of α-SMA immunolabeling around periportal areas (Fig. 7b). Masson's trichrome showed that collagen deposition in the triads was comparable with α-SMA-immunolabeled cell localization (Fig. 7c, d).

In normal livers, antidesmin immunolabeling highlighted the presence of a delicate desmin-positive network of perisinusoidal spindle-shaped cells (Fig. 7e, f). In livers with fibrosis, there was an accumulation of desmin-positive cells in the periportal areas, which was associated with a lack of desmin-positive cells within the sinusoidal spaces (Fig. 7g, h).

Anti-MT immunolabeling of normal alligator skin revealed a diffuse granular cytoplasmic labeling of keratinocytes and dermal fibroblasts (Fig. 8a). Anti- MT immunolabeling was markedly reduced in the cytoplasm of keratinocytes and fibroblasts of alligators with DS (Fig. 8b). Immunolabeling was absent in sections incubated with isotype control antibodies (Supplemental Figures S2d–f).

Discussion

Scales are skin appendages evolved by reptiles, which exquisite arrangement pattern has made crocodilian leather one of the most demanded products of the luxury fashion market since 1800.[7,21] The DS defect undermines the appeal of the belly scale pattern with an array of defects, including focal to extensive pitting and roughening of the cranial and medial edge of the belly, brown discoloration, and a linear, ring-shaped indentation on the central portion of the scale in severe cases. This indentation translates into linear defects of processed leather (crust tan skin). Histologically, depression of the epidermis and superficial dermis corresponded to the gross indentation. A key microscopic feature of DS was significant orthokeratosis associated with atrophy of the live strata of the epidermis. Compared with controls, the average thickness of β-corneal layer at the level of the plate was almost doubled, while the α-corneal layer was four-times increased. DS lesions also had loss of

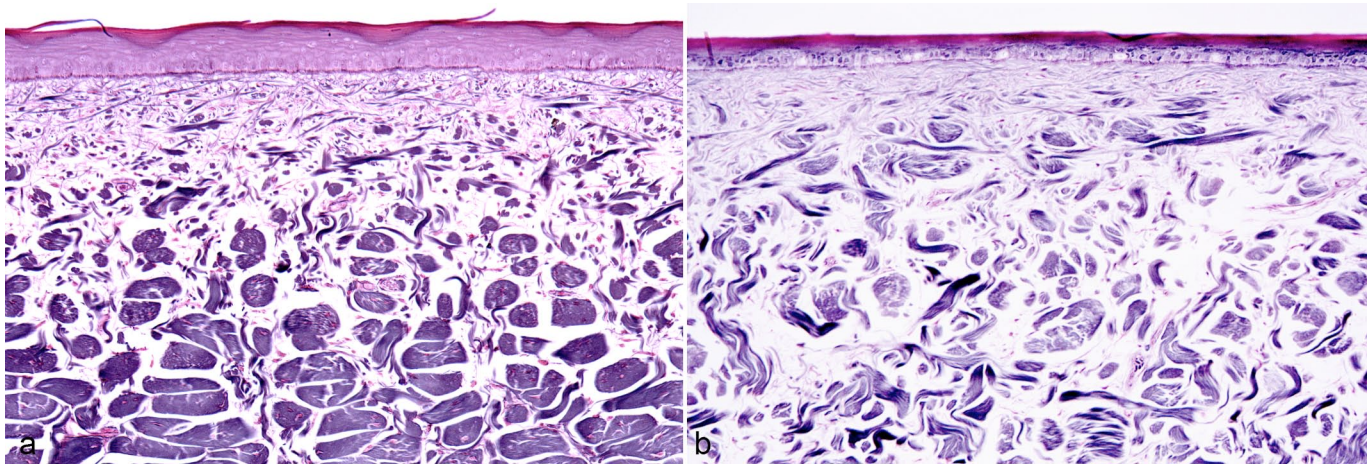

Figure 5. Dermal collagen organization, skin, American alligator. Reticulin stain. (a) Normal anatomy of alligator dermis showing an orderly arrangement of collagen bundles that became larger in the deep dermis. Note that all bundles are oriented perpendicular to the cut section and the separation between the superficial and deep dermis is well-defined. (b) In double scales, collagen bundles are reduced in size and are separated by an increase in ground matter. The bundles are arranged haphazardly and a clear definition between superficial and deep dermis is lost.

Table 1. Micronutrient concentration in liver and serum of alligators with liver fibrosis compared with alligators with normal livers.

	Hepatic Levels (μg/g)					Serum Levels (mg/ml)				
	Control (n = 22)		Liver Fibrosis (28)			Control (n = 22)		Liver Fibrosis (28)		
	Mean (SD)	SD	Mean (SD)	P Value	Trend	Mean (SD)	SD	Mean (SD)	P Value	Trend
Vitamin A	389.8	251.4	880.6 (441.1)	****						
Palmitate	362	242.8	855.1 (447.7)	****						
Retinol	28.71	16.63	41.73 (44.56)					0.07 (0.01)		
Iron	388.2	134.6	734.6 (327)	****		136.2	62.25	182.1 (101.2)		
Zinc	81.27	13.9	96.73 (26.79)	*		1	0.13	0.62 (0.19)	****	
Copper	39.36	14.52	57.92 (56.64)			0.67	0.13	0.55 (0.17)	*	
Selenium	2.92	0.48	3.37 (0.72)			324.9	67.44	353.6 (42.02)		
Manganese	5.44	2.08	3.42 (0.86)	****		8.21	3.24	10.45 (4.88)	*	
Molybdenum	0.29	0.09	0.13 (0.09)			19.09	4.66	22.48 (7.1)		
Cobalt	0.02	0.01	0.02 (0.01)			0.28	0.28	0.72 (1.22)		
Arsenic	0.09	0.07	0.1 (0.07)			0.01	0	0.02 (0)		
Cadmium	0.02	0	0.02 (0.01)			0.1	0	0.1 (0)		
Thallium	0.02	0	0.02 (0.01)			0.1	0	0.1 (0)		
Lead	0.04	0.17	0.02 (0.05)			0.01	0	0.01 (0)		
Vitamin E	69	28.36	57.62 (31.42)			4.95	2.41	3.4 (1.52)	**	

Abbreviation: n, number of samples; SD, standard deviation.
Difference between means was calculated by Student's t-test. For nonparametric sets, difference of medians was calculated by Mann-Whitney test.
Significant results with P value $<$ .0001 are marked as ****, P value = .0021 as **, and P value $<$ .05 as*.

the characteristic compactness of the reptilian β-keratinized corneal layer, with frequent fragmentation of keratin, which corresponded grossly to the roughened pitted areas of the scale. Finally, collagen bundle disarray was evident in the superficial to deep dermis of several DS individuals (9/19; 47%).

To further understand the pathogenesis of DS we examined histological samples of organs from the DS 2018 and Control 2019 alligator cohorts. This showed a high incidence of hepatic fibrosis (69%) in the DS 2018 cohort of alligators while liver disease was not seen in the control cohorts. Interestingly, hepatic fibrosis was always present in alligators that had gross evidence of DS (18/18; 100%). There is little information available on normal liver histology of reptiles, and to the best of our knowledge, hepatic fibrosis has not been previously described in alligators. Hepatic fibrosis represents a scarring response to chronic liver injury after a variety of insults.[20] Other hepatic changes noted histologically in the DS 2018 cohort were bile duct proliferation, glycogen accumulation causing hepatocytes vacuolation and often swelling, and increased numbers of periportal melanomacrophages. Bile duct proliferation is considered a

Table 2. Composition of the feed stocks administered to alligators during the study.

	Unit	Feed 2018	*N*	Feed 2019	*N*	*P* Value
Vitamin A	IU/100 g	3193	19	1521	21	****
Iron	ppm	1197	19	605	21	****
Copper	ppm	36	19	20	21	****
Manganese	ppm	133	19	78	21	****
Zinc	ppm	373	19	236	21	****
Sulfur	%	0.66	19	0.79	21	
Phosphate	%	1.61	19	1.28	21	
Potassium	%	0.73	19	0.77	21	
Magnesium	%	0.13	19	0.13	21	
Calcium	%	2.85	19	1.82	21	****
Sodium	%	0.49	19	0.33	21	
Fiber	%	0.7	19	1.3	21	**
Fat	%	6.9	19	14.6	21	****
Protein	%	55	19	50	21	****
Tryptophan	%	0.53	19	0.6	13	
Arginine	%	3.1	19	2.91	13	
Histidine	%	1.5	19	1.27	13	
Lysine	%	3.4	19	3.3	13	
Phenylalanine	%	2.5	19	2.35	13	
Tyrosine	%	1.6	19	1.36	13	
Leucine	%	4.3	19	4.25	13	
Isoleucine	%	2	19	1.99	13	
Methionine	%	0.9	19	1.22	13	
Valine	%	2.8	19	2.7	13	
Cystine	%	0.99	19	0.87	13	
Alanine	%	3.1	19	3.12	13	
Glycine	%	3.3	19	3.35	13	
Proline	%	3.2	19	3.31	13	
Glutamic acid	%	6.6	19	6.93	13	
Serine	%	2.4	19	2.6	13	
Threonine	%	1.8	19	2.17	13	
Aspartic acid	%	4	19	4.21	13	

Abbreviation: *N*, number of samples analyzed.
Difference between means was calculated by Student's *t*-test.
Significant results with *P* value $<$ .0001 are marked as ****, *P* value = .0021 as **.

nonspecific reaction to liver injury in humans and several domestic species.[41] Glycogen accumulation, with the exception of storage prior to hibernation, is often considered a consequence of disturbance of glucose homeostasis in hepatocytes of fish,[38] amphibians,[3] and mammalians.[10,42] We suggest that a similar mechanism is occurring in alligators.

An increase of pigment-laden macrophages (melanomacrophages) was also evident. While an enhanced phagocytic activity of Kupffer cells due to increased hepatocyte loss is a possible differential,[31,36] several other conditions and factors can cause this.[34]

Myofibroblasts are considered the main source of collagen production in liver fibrosis in humans, mice, and dogs.[12,18] These are fibroblast-like cells that express α-SMA, which confers contractile properties.[18] As expected, immunolabeling of alligator livers with hepatic fibrosis showed α-SMA-positive cell numbers were markedly increased around periportal areas, where the collagen accumulated. Myofibroblasts can be recruited in livers by activation of hepatic stellate cells (or Ito cells), from liver resident fibroblasts (portal or centrilobular), epithelial cells that undergo epithelial-to-mesenchymal transition, bone marrow-derived fibrocytes, and from smooth muscle cells that surround blood vessels.[15] Comparison of α-SMA and desmin immunolabeling between normal alligator livers and livers with periportal fibrosis suggests that hepatic fibrogenic myofibroblast cells are derived from proliferation of periportal and perivascular fibroblasts and also by recruitment of desmin-positive cells from the sinusoids. The latter are considered most likely to be hepatic stellate cells.

Causes of progressive liver fibrosis include chronic viral infection, prolonged use of hepatotoxic drugs, longstanding exposure to aflatoxin, iron and copper accumulation, chronic biliary cholangitis, autoimmune hepatitis, and chronic vitamin A toxicity.[13,18,42] Alcohol abuse, nonalcoholic fatty liver

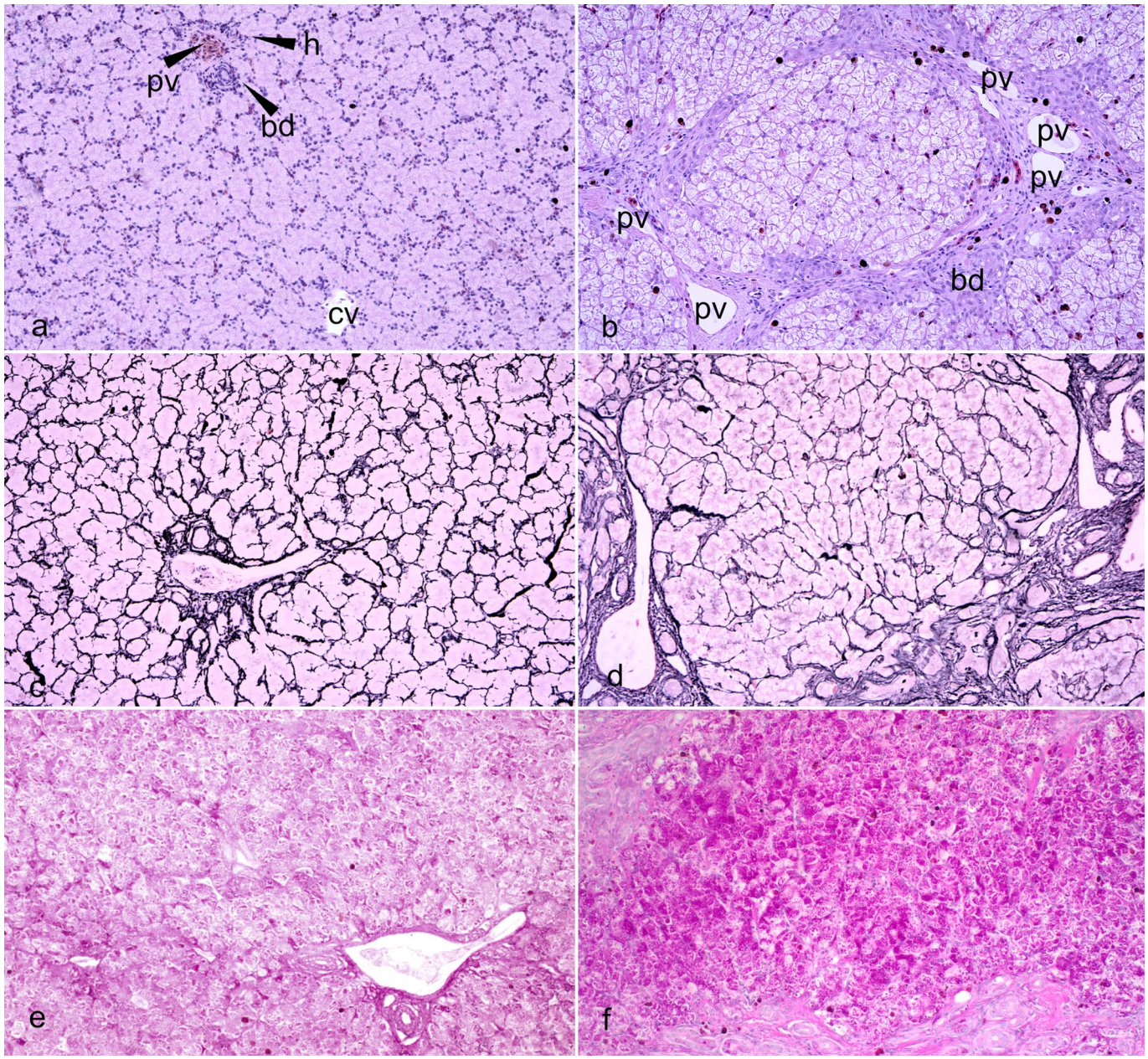

Figure 6. Liver, American alligator. (a) Normal liver. Normal lobule architecture showing a triad (upper left) composed of 1 portal vein (pv), 1 hepatic artery (h), and a biliary duct (bd). A central vein (cv) is seen at the center of the lobule. Hematoxylin and eosin (HE) (b). Liver of an alligator with double scale affected by severe fibrosis showing bands of collagen fibers bridging between several triads associated with increased numbers of melanin-laden macrophages. Biliary ducts (bd) are increased in number and are tortuous. Portal veins (pv) are tortuous and irregularly dilated. Hepatocytes show diffuse vacuolation and swelling. The central vein is collapsed. HE. (c) Regular pattern of reticulin fibers in the control liver. Reticulin stain. (d) Nodular distortion of the hepatic lobule in the liver of an alligator with double scale with severe fibrosis. Reticulin stain. (e) Normal glycogen accumulation in control liver. Periodic acid-Schiff (PAS). (f) Increased glycogen accumulation in the fibrotic liver of an alligator with double scale. PAS.

disease, and nonalcoholic steatohepatitis are largely reported in humans.[16] In the alligator livers examined, infectious causes were considered unlikely due to the lack of histological evidence of underlying cholangiohepatitis, or bacterial or viral infections. Considering the distribution of the liver disease within the examined population (animals of various ages, sexes, and from all enclosures were impacted) and the histological pattern of liver pathology, a chronic toxic insult underlying the liver injury was suspected.

Toxic causes of liver disease leading to fibrosis, such as chronic exposure to aflatoxin and carbon tetrachloride, were excluded based on routine toxicological testing of feed and water. Vitamin A, copper, and iron, which are known to be hepatotoxic in high doses, were found to be significantly increased

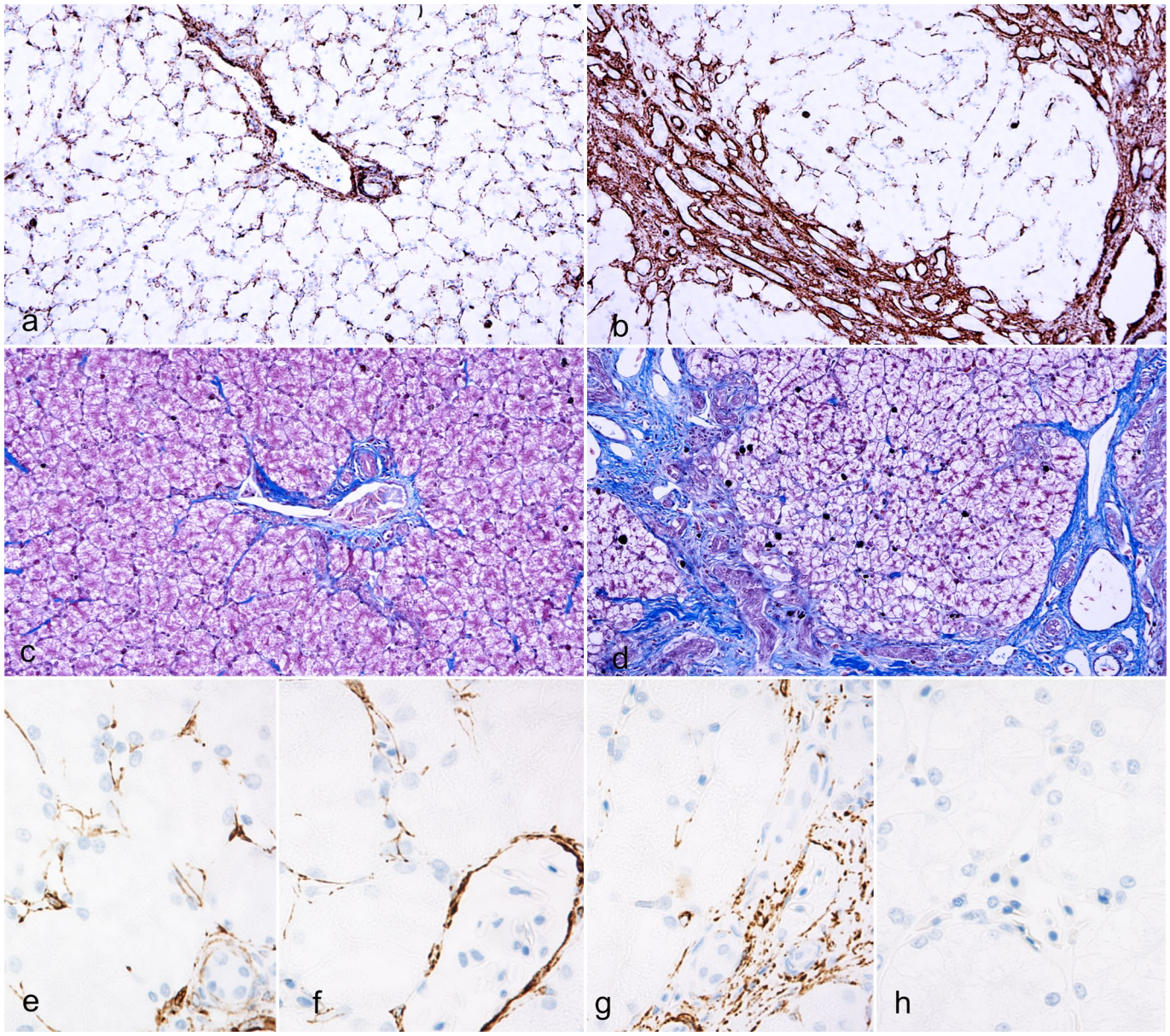

Figure 7. Distribution of α-smooth muscle actin (α-SMA) positive cells, collagen, and desmin-positive cells, liver, American alligator. (a) In normal livers, α-SMA-positive myofibroblasts are evenly distributed throughout perisinusoidal spaces and form a thin rim around vessels and biliary ducts in the portal areas. α-SMA immunohistochemistry (IHC). (b) In a fibrotic liver from an alligator with double scale, α-SMA-positive myofibroblasts are increased within periportal areas. Note the numbers of myofibroblasts in the perisinusoidal spaces are reduced compared with normal livers. α-SMA IHC. (c) Collagen distribution in a normal liver. Masson's trichrome. (d) In a fibrotic liver from an alligator with double scale, increased collagen deposition localizes in periportal areas where α-SMA-positive cells concentrate. Masson's trichrome. (e) In normal livers, desmin-positive cells are evenly distributed within perisinusoidal spaces in both periportal areas and (f) centrilobular areas. Desmin IHC. (g) In a fibrotic liver from an alligator with double scale, desmin-positive cells accumulate in the periportal areas, (h) while they are depleted from the midzonal and centrilobular areas. Desmin IHC.

in the Feed 2018, which composed the diet of DS 2018 cohort alligators. Notably, 32,000 IU/kg of vitamin A was found in the Feed 2018, which is almost double the recommended level for crocodilians (12,000–17,000 IU/kg).[1,19] Liver damage related to chronic hypervitaminosis A is a rare, but is a well-described condition in humans[30] and has been reported once in a cat.[17] Although occasionally suspected in pet reptiles, it has not been fully characterized.[35] The pathologic changes in the liver in humans and the cat are related to increased retinyl storage in the organ, which may result in portal hypertension, secondary to sinusoidal compression, and hyperplasia of stellate cells followed by fibrosis.[16,33]

The liver serves as the primary storage site for vitamin A, predominantly in the form of retinyl esters.[4,8] In alligators, vitamin A is primarily stored as retinyl palmitate. In cases of fibrosis in alligator livers, the average concentration of vitamin A

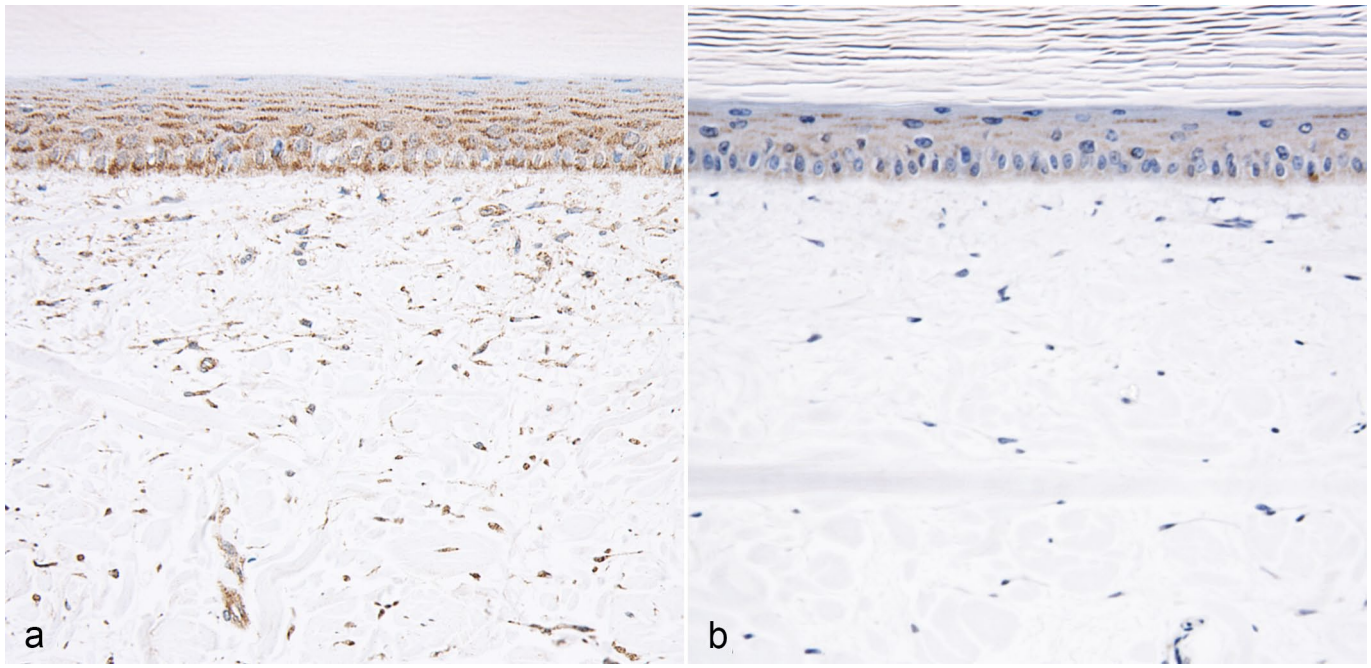

Figure 8. Antimetallothionein immunohistochemistry (IHC), skin, American alligator. (a) Normal scale. Metallothionein is labeled in a diffuse, granular cytoplasmic pattern in all layers of the live epidermis and dermal fibroblasts. (b) Scant metallothionein immunolabeling is detectable in the keratinocytes and dermal fibroblasts of animals with double scale.

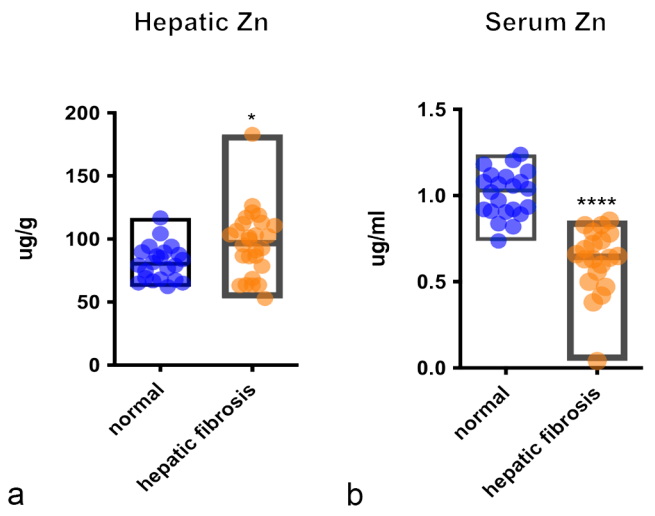

Figure 9. Hepatic and serum levels of zinc. Box graphs show levels of (a) hepatic and (b) serum zinc in alligators with liver fibrosis (n = 28) compared with alligators with normal livers (n = 22). Central line in the box indicates mean. Difference of means was calculated by Student's t-test. Significant differences are indicated with **** for with P value < .0001 and * for P value < .05.

was found to be double that of normal alligator livers. This concentration was also much higher than hepatic vitamin A levels for other carnivorous reptiles, typically around 300 µg/g (100 IU/g).[35] This result raised the suspicion of vitamin A toxicity. In addition, a positive correlation was observed between the severity of liver fibrosis and the concentration of hepatic vitamin A in alligators. This correlation lends support to the hypothesis that vitamin A toxicity could be a potential cause of liver disease in this case.

Recommended levels of copper and iron for crocodilian diets vary in the literature.[19] While copper levels in feed 2018 were higher than feed 2019, the levels were within recommended ranges (8–100 ppm). However, iron levels were considerably higher than recommended range (27–875 ppm).[19] The toxicity of copper and iron excess is characterized by the production of reactive oxygen species, causing lipid peroxidation reactions that damage cellular organelles and membranes,[42] which result in hepatocyte damage. Copper toxicity is especially common in sheep and in several dog breeds with genetic defects of copper metabolism.[42] In this study, alligators' hepatic copper levels were increased in cases with fibrosis compared with normal livers, although this variation was not statistically significant. Rhodanine stain, performed to highlight copper loading in fibrotic livers, was negative (data not shown). Also, serum levels of copper were lower in alligators with liver fibrosis than controls. Hemochromatosis, also known as iron storage disease, is defined by increased iron deposition in many tissues leading to organ toxicosis. Characteristic lesions of hemochromatosis include hepatocellular and macrophagic iron loading in association with liver injury and iron deposition in other sites (intestinal lamina propria, myocardium, spleen, pancreas, or kidney).[40] While rare in domestic animals,[10] hemochromatosis is quite common in some captive nectar and fruit-eating birds species, such as toucans and lorikeets, while it is infrequent in parrots[40] and has recently been described in kori bustards.[9] In the alligators in this study, iron levels were

significantly increased in fibrotic livers, and were positively correlated to the severity of fibrosis. However, the mesenchymal pattern of iron accumulation, the lack of stainable iron in hepatocytes and other tissues, and the normal iron serum levels suggest that the origin of iron loading was more likely secondary to hepatocyte loss rather than chronic dietary intake.[11] Considering these findings, copper and iron were deemed less likely than vitamin A to be the inciting cause of liver damage in this study; however, their contribution to liver disease cannot be completely excluded. Further toxicological studies are warranted to investigate the toxic ranges of vitamin A, iron, and copper in crocodilians.

While an association between DS defects and hepatic fibrosis is clear in this study, the pathogenesis of DS and how it relates to liver disease is not. It is important to consider the potential contributions that increased dietary levels of vitamin A may have had on the development of DS. In fact, the main recognized effect of vitamin A is in maintaining normal epithelial tissues. Among reptiles, acute vitamin A toxicity is reported in chelonians, where it manifests with skin scaling often progressing to extensive necrosis of the epithelium.[29] The chronic effects of vitamin A toxicity on reptilian skin have never been reported. Serum retinol levels, which are commonly used as biomarker for vitamin A levels,[29] were an average of 0.07 µg/ml in alligators with hepatic fibrosis. Although these values correspond to the lower range of values reported for the species,[26] we were unable to compare with an internal reference range, as we lacked the serum levels for control alligators. Unfortunately, the role of vitamin A in DS development remains unclear.

A possible link between DS and hepatic fibrosis may relate to the imbalance between hepatic accumulation and systemic distribution of several elements in alligators with hepatic fibrosis. Specifically, vitamin E, copper, and zinc were significantly decreased in the serum of DS alligators, although their hepatic concentrations remained constant or, like zinc, slightly increased. Manganese instead was significantly increased in the serum and depleted in the liver. Of all serum micronutrient imbalances in alligators, zinc reduction was the most striking given its severity and statistical significance compared with controls. Since cutaneous lesions are common manifestations of zinc deficiency both in humans and domestic animals, and are commonly reported in humans with chronic liver disease,[16] we investigated whether zinc deficiency could be contributing to DS in alligators. MT expression may be used for subjective determination of zinc concentrations in skin samples.[32] MTs are cysteine-rich, zinc-binding proteins synthesized in response to tissue zinc levels.[24] Anti-MT immunolabeling of alligator skin revealed a drastic reduction in MTs in alligators with DS and liver fibrosis, supporting the hypothesis of zinc deficiency as a potential cause of skin lesions in these animals. Beside their primary role in zinc metabolism, MTs are also involved in copper storage and exchange.[24] Considering this, it is also possible that low serum levels of copper may have contributed together with the low serum zinc levels to the markedly reduced immunolabeling of MTs in skin with DS.

Conclusions

This study shows a correlation between liver disease and the skin quality of farmed alligators. DS is considered anecdotally as a multifactorial skin condition. Our results suggest that DS can result from a series of nutritional imbalances especially in diets with high levels of vitamin A and iron, and that zinc deficiency likely plays a role. Lower zinc levels were paradoxical, developing in alligators with higher hepatic and dietary levels of zinc compared with controls. As the liver is the main organ responsible for the zinc metabolism,[16] liver diseases could be responsible for zinc deficiency in this case. There is limited knowledge on the nutritional needs of captive crocodilians. The results of this study indicate that the current recommended dietary vitamin A concentrations between 12,000 and 17,000 UI/kg are safe, while higher concentrations administered over months may be hepatotoxic in crocodilians. Similarly, levels of copper and iron appear to be safe at the respective doses of 20 and 600 ppm. Finally, zinc concentration at 236 ppm in crocodilian diets seems adequate.

Acknowledgments

We thank Lynn Stevenson and Frazer Bell, Veterinary Diagnostic Services, College of Medical, Veterinary & Life Sciences, School of Veterinary Medicine, University of Glasgow; Marcus Reddell, Tallowcreek Ranch, Texas; Susan Peters and Brian Cloak, University College Dublin, School of Veterinary Medicine for their technical support. We also thank Dr Catherine Barr, Maritza Anguiano, Texas Veterinary Medical Diagnostic Laboratory and Dr Peter O'Brien, University College Dublin, School of Veterinary Medicine for their contributions to the clinical investigation. We also thank Prof. Lorenzo Alibardi, Dipartimento di Scienze Biologiche, Geologiche e Ambientali Università di Bologna, for his support on the development of immunohistochemical protocols and Prof. Joseph Cassidy University College Dublin, School of Veterinary Medicine for the critical review of the manuscript.

Declaration of Conflicting Interests

The author(s) declared no potential conflicts of interest with respect to the research, authorship, and/or publication of this article.

Funding

The author(s) received no financial support for the research, authorship, and/or publication of this article.

ORCID iDs

Ilaria M. Piras https://orcid.org/0000-0003-0852-7336
Pamela A. Kelly https://orcid.org/0000-0002-3047-8465

References

1. Ariel E, Ladds PW, Buenviaje GN. Concurrent gout and suspected hypovitaminosis A in crocodile hatchlings. *Aust Vet J*. 1997;**75**:247–249.
2. Bazin I, Nabais E, Lopez-Ferber M. Rapid visual tests: fast and reliable detection of ochratoxin A. *Toxins (Basel)*. 2010;**2**:2230–2241.
3. Bernabo I, Biasone P, Macirella R, et al. Liver histology and ultrastructure of the Italian newt (*Lissotriton italicus*): normal structure and modifications after acute exposure to nonylphenol ethoxylates. *Exp Toxicol Pathol*. 2014;**66**:455–468.

4. Blomhoff R, Green MH, Berg T, et al. Transport and storage of vitamin A. *Science*. 1990;**250**:399–404.
5. Brien ML, Webb GJ, McGuinness K, et al. The relationship between early growth and survival of hatchling saltwater crocodiles (*Crocodylus porosus*) in captivity. *PLoS ONE*. 2014;**9**:e100276.
6. Buenviaje G. *Studies on Skin Diseases of Crocodiles*. Thesis. Australia: James Cook University of North Queensland; 2000.
7. Chang C, Wu P, Baker RE, et al. Reptile scale paradigm: Evo-Devo, pattern formation and regeneration. *Int J Dev Biol*. 2009;**53**:813–826.
8. Clugston RD, Blaner WS. Vitamin A (retinoid) metabolism and actions: what we know and what we need to know about amphibians. *Zoo Biol*. 2014;**33**:527–535.
9. Cudd SK, Garner MM, Cartoceti AN, et al. Hepatic lesions associated with iron accumulation in captive kori bustards (*Ardeotis kori*). *Vet Pathol*. 2022;**59**:164–168.
10. Cullen JM, Stalker MJ. Liver and biliary system. In: Maxie MG, ed. *Jubb, Kennedy & Palmer's Pathology of Domestic Animals: Volume 2*. 6th ed. St. Louis, MO: W.B. Saunders; 2016:258–352.e251.
11. Deugnier Y, Turlin B. Pathology of hepatic iron overload. *Semin Liver Dis*. 2011;**31**:260–271.
12. Eulenberg VM, Lidbury JA. Hepatic fibrosis in dogs. *J Vet Intern Med*. 2018;**32**:26–41.
13. Fox R, Stace N, Wood K, et al. Liver toxicity from vitamin A. *JGH Open*. 2020;**4**:287–288.
14. Gigante JM. Tannage et gestion de la qualité des peaux de crocodiliens au nord du 45ème parallèle. In: Proceedings of the 18th Working Meeting of the IUCN-SSC Crocodile Specialist Group; 2006; IUNC, Gland, Switzerland.
15. Gressner OA, Rizk MS, Kovalenko E, et al. Changing the pathogenetic roadmap of liver fibrosis? Where did it start; where will it go? *J Gastroenterol Hepatol*. 2008;**23**:1024–1035.
16. Grungreiff K, Reinhold D, Wedemeyer H. The role of zinc in liver cirrhosis. *Ann Hepatol*. 2016;**15**:7–16.
17. Guerra JM, Daniel AG, Aloia TP, et al. Hypervitaminosis A-induced hepatic fibrosis in a cat. *J Feline Med Surg*. 2014;**16**:243–248.
18. Higashi T, Friedman SL, Hoshida Y. Hepatic stellate cells as key target in liver fibrosis. *Adv Drug Deliv Rev*. 2017;**121**:27–42.
19. Isberg SR. Nutrition of juvenile saltwater crocodiles (Crocodylus porosus) in commercial production systems. *CAB Rev*. 2007;**2**(91):1–11.
20. Jiao J, Friedman SL, Aloman C. Hepatic fibrosis. *Curr Opin Gastroenterol*. 2009;**25**:223–229.
21. Joanen T, McNease L, Elsey RM, et al. The commercial consumptive use of the American alligator (*Alligator mississippiensis*) in Louisiana: its effect on conservation. In: Freese CH, ed. *Harvesting Wild Species: Implications for Biodiversity Conservation*. Baltimore, MD: Johns Hopkins University Press; 1997:349–374.
22. Joanen T, Merchant M. The history and development of the alligator industry: a historical perspective. In: Henke SE, Eversole CB, eds. *American Alligators: Habitats, Behaviors, and Threats*. New York, NY: Nova Science Publications; 2018:349–374.
23. King FW, Messel H, Ross JP, et al. *Crocodiles: An Action Plan for Their Conservation*. Gland, Switzerland: IUCN; 1992.
24. Krezel A, Maret W. The bioinorganic chemistry of mammalian metallothioneins. *Chem Rev*. 2021;**121**:14594–14648.
25. Kushlan JA, Mazzotti FJ. Population biology of the American crocodile. *J Herpetol*. 1989;**23**:7–21.
26. Lance VA, Morici LA, Elsey RM, et al. Hyperlipidemia and reproductive failure in captive-reared alligators: vitamin E, vitamin A, plasma lipids, fatty acids, and steroid hormones. *Comp Biochem Physiol B Biochem Mol Biol*. 2001;**128**:285–294.
27. Manolis SC, Webb GJW. *Best Management Practices for Crocodilian Farming* (Vol. 2023). Darwin, NA, Australia: IUCN-SSC Crocodile Specialist Group; 2016.
28. Manolis SC, Webb GJW. *Tracking Crocodile Skin Defects: From Farm to Product*. Canberra: Australian Government, Rural Industries Research and Development Corporation; 2011.
29. Mans C, Braun J. Update on common nutritional disorders of captive reptiles. *Vet Clin North Am Exot Anim Pract*. 2014;**17**:369–395.
30. Nollevaux MC, Guiot Y, Horsmans Y, et al. Hypervitaminosis A-induced liver fibrosis: stellate cell activation and daily dose consumption. *Liver Int*. 2006;**26**:182–186.
31. Ribeiro HJ, Procopio MS, Gomes JM, et al. Functional dissimilarity of melanomacrophage centres in the liver and spleen from females of the teleost fish *Prochilodus argenteus. Cell Tissue Res*. 2011;**346**:417–425.
32. Romanucci M, Bongiovanni L, Russo A, et al. Oxidative stress in the pathogenesis of canine zinc-responsive dermatosis. *Vet Dermatol*. 2011;**22**:31–38.
33. Shirakami Y, Lee SA, Clugston RD, et al. Hepatic metabolism of retinoids and disease associations. *Biochim Biophys Acta*. 2012;**1821**:124–136.
34. Stacy BA, Pessier APP, Ossiboff RJ. Host response to infectious agents and identification of pathogens in tissue sections. In: E Jacobson, & M Garner, eds. *Infectious Diseases and Pathology of Reptiles*. Boca Raton: CRC Press; 2020: 257–297.
35. Stahl SJ. Hypervitaminosis A. In: Jörg M, Thomas MD, eds. *Clinical Veterinary Advisor*. St. Louis, MO: W.B. Saunders; 2013:108–110.
36. Steinel NC, Bolnick DI. Melanomacrophage centers as a histological indicator of immune function in fish and other Poikilotherms. *Front Immunol*. 2017;**8**:827.
37. Temsiripong Y, Woodward AR, Ross JP, et al. Survival and growth of American alligator (Alligator mississippiensis) hatchlings after artificial incubation and repatriation. *J Herpetol*. 2006;**40**:415–423.
38. Thophon S, Pokethitiyook P, Chalermwat K, et al. Ultrastructural alterations in the liver and kidney of white sea bass, Lates calcarifer, in acute and subchronic cadmium exposure. *Environ Toxicol*. 2004;**19**:11–19.
39. Thorbjarnarson J. Crocodile tears and skins: international trade, economic constraints, and limits to the sustainable use of crocodilians. *Conser Biol*. 1999;**13**:465–470.
40. Trupkiewicz J, Garner MM, Juan-Sallés C. Passeriformes, caprimulgiformes, coraciiformes, piciformes, bucerotiformes, and apodiformes. In: Terio KA, McAloose D, Leger JS, eds. *Pathology of Wildlife and Zoo Animals*. Washington, DC: Academic Press; 2018:799–823.
41. Van Den Ingh TSGAM, Van Winkle T, Cullen JM, et al. Morphological classification of parenchymal disorders of the canine and feline liver. In: Rothuizen J, Bunch SE, Charles JA eds. *WSAVA Standards for Clinical and Histological Diagnosis of Canine and Feline Liver Diseases*. St. Louis, MO: Elsevier Saunders; 2006:77–83.
42. Van Wettere AJ, Brown DL, Cullen J. Hepatobiliary system and exocrine pancreas. In: Zackary JF, ed. *Pathologic basis of Veterinary Disease*. St. Louis, MO: Elsevier; 2016:412–470.
43. Webster JD, Solon M, Gibson-Corley KN. Validating immunohistochemistry assay specificity in investigative studies: considerations for a weight of evidence approach. *Vet Pathol*. 2021;**58**:829–840.
44. Wells MY, Weisbrode SE, Maurer JK, et al. Variable hepatocellular vacuolization associated with glycogen in rabbits. *Toxicol Pathol*. 1988;**16**:360–365.